Distribution of Spectral Lags in Gamma Ray Bursts

Li Chen¹

Department of Astronomy, Beijing Normal University, Beijing 100875, P.R. China

chenli@bnu.edu.cn

Yu-Qing Lou²

(a) Physics Department and the Tsinghua Center for Astrophysics (THCA), Tsinghua University, Beijing 100084, China; (b) Department of Astronomy and Astrophysics, The University of Chicago, 5640 South Ellis Avenue, Chicago, IL 60637 USA; (c) National Astronomical Observatories, Chinese Academy of Sciences, A20, Datun Road, Beijing 100012, The People's Republic of China

louyq@mail.tsinghua.edu.cn and lou@oddjob.uchicago.edu

Mei Wu³

Particle Astrophysics Laboratory, Institute of High Energy Physics, Chinese Academy of Sciences, Beijing 100039, The People's Republic of China

Jin-Lu $\mathrm{Qu}^3,$ Shu-Mei Jia^1 and Xue-Juan Yang^1

ABSTRACT

Using the data acquired in the Time To Spill (TTS) mode for long gamma-ray bursts (GRBs) collected by the Burst and Transient Source Experiment on board the Compton Gamma Ray Observatory (BATSE/CGRO), we have carefully measured spectral lags in time between the low ($25-55~{\rm keV}$) and high ($110-320~{\rm keV}$) energy bands of individual pulses contained in 64 multi-peak GRBs. We find that the temporal lead by higher-energy γ -ray photons (i.e., positive lags) is the norm in this selected sample set of long GRBs. While relatively few in number, some pulses of several long GRBs do show negative lags. This distribution of spectral lags in long GRBs is in contrast to that in short GRBs. This apparent difference poses challenges and constraints on the physical mechanism(s) of producing long and short GRBs. The relation between the pulse peak count rates and the spectral lags is also examined. Observationally, there seems to be no clear evidence for systematic spectral lag-luminosity connection for pulses within a given long GRB.

Subject headings: Gamma-rays: bursts — gamma-rays: observations — plasmas — radiation mechanism: general — methods: data analysis — shock waves

1. Introduction

Temporal delays in the arrival of low-energy photons relative to that of high-energy photons are well known in the spectra of gamma-ray bursts (GRBs). Link, Epstein & Priedhorsky (1993) used the autocorrelation analysis to investigate temporal properties of GRBs in different energy bands. Cheng, Ma, Cheng, Lu & Zhou (1995) first quantified the time delay of GRBs in the soft energy band. Fenimore & Zand (1995) found that the average autocorrelation of GRB temporal histories is a universal function that can measure the timescale as a function of energy. The dependence is a power law in energy with an index of ~ 0.4 . This is the first quantitative relationship between temporal and spectral structures in GRBs. Band (1997) performed a cross-correlation analysis on a sample of 229 strongest BATSE GRBs to demonstrate that the hard-to-soft spectral evolution is generic in most bursts. Norris, Marani & Bonnell (2000) estimated spectral lags between the light curves of 6 GRBs with known redshifts z in the energy ranges of the BATSE channel 3 (100-300 keV) and channel 1 (25-50 keV), concluding that the pulse peak luminosity and the spectral lag τ_{lag} in time anticorrelate with each other and may well be fit with a power law $L_{53} \approx 1.3(\tau_{lag}/0.01s)^{-1.15}$ where L_{53} is the GRB luminosity in unit of 10^{53} erg s⁻¹. This appears to be the first valuable although preliminary information for GRB luminosity based on spectral and temporal properties of gamma-ray observations alone. Another tentative GRB luminosity indicator is the empirical relation between luminosity and variability first proposed by Fenimore & Ramirez-Ruiz (2000), indicating a correlation between spectral lags and V (variability) parameter. This correlation was further demonstrated by Schaefer, Deng & Band (2001) by systematically examining the available BATSE data of τ_{lag} and of V for 112 GRBs. By extrapolating the lagluminosity relation of GRBs (Ioka & Nakamura 2001), Murakami, Yonetoku, Izawa & Ioka (2003) further inferred the star-formation history in the universe out to redshift $z \sim 4$.

The lag-luminosity relation or the variability-luminosity relation might make GRBs into standard candles as cosmological distance indicator. This does not mean that all GRBs have the same luminosity. In this context, let us look at the cases of Cepheid variables and Type Ia supernovae (SNe Ia). The well-established period-luminosity relation of Cepheid variables allows us to know their intrinsic luminosities from periodicities in their light curves. Similarly, the decline rate of the light curve of a SN Ia may determine its peak luminosity after some corrections and adjustments (Phillips 1993; see extensive references in Niemeyer & Truran 2000). Now the lag/V-luminosity relation might offer a possibility of estimating a GRB luminosity based on GRB observations alone. The cosmological significance of this potential Cepheid-like relation is self-evident. Comparing with SNe Ia as cosmological distance indicators, GRB cosmology has at least three apparent advantages (Norris 2003; Dai, Liang & Xu 2004): (1) much larger redshift z range; (2) much weaker effects of dust extinction; and (3) weaker possible luminosity evolution with redshift z. Fenimore & Ramirez-Ruiz (2000) take the lead in estimating the redshifts z for 220 bright, long duration BATSE GRBs by using V-luminosity relation. Norris (2002) used a two-branch lag-luminosity relationship to yield the number distribution of GRBs in luminosity, distance, and redshift z. It is further inferred that some GRBs are identified to concentrate near the local galactic superplane, including GRB 980425 which was known to associate with a supernova. Applying the lag-luminosity relation to 1218 GRBs with positive lags, hardness ratios, peak fluxes and durations, Band, Norris & Bonnell (2003) compiled an extensive catalog for GRBs redshifts. Dai et al. (2004) attempted to constrain the mass density of the universe and the nature of dark energy with a sample of 12 GRBs with known redshifts, peak energies and break times of afterglow light curves. Their results are consistent with those from SNe Ia. Undoubtedly, a larger sample expected from the upcoming SWIFT satellite may provide further clues and constraints.

There have been several attempts to interpret the empirical relations for luminosity versus spectral lag or V in GRB observations. Salmonson (2000, 2001) proposed that these correlations might be caused by the variety, among GRBs, of relativistic velocities at which emitting regions move toward the observer. He introduced the peak number luminosity N_{pk} (i.e., photons s⁻¹) instead of the peak luminosity L_{pk} . With this characterization, he not only reproduced the result of Norris et al. (2000), namely $L_{pk} \propto \tau_{lag}^{-1.15}$ but also obtained a better fit for the equivalent relation $N_{pk} \propto \tau_{lag}^{-0.98}$. For a burst expanding with a Lorentz factor $\gamma \gg 1$, he educed $N_{pk} \propto \tau_{lag}^{-1}$. In terms of the energy conservation when the radiative cooling dominates, Schaefer (2004) considered that the average cooling rate per particle in the emitting region of the jet should be either equal to the total luminosity L_{tot} over the number of emitting particles (roughly $\sim M_{jet}/m_{proton}$) or the time derivative of the mean particle energy E_{pk} , that is: $\dot{E}_{pk} = -L_{tot}/(M_{jet}/m_{proton})$. Using the relation $L_{tot} = L_{pk}\Omega/(4\pi)$, where $\Omega \approx \pi \gamma^2$ is the solid angle into which the radiation is beamed at, and evaluating \dot{E}_{pk} by $[E_{pk}(T_1) - E_{pk}(T_3)]/(T_1 - T_3) \propto \tau_{lag}^{-1}$, they derived the following relation $L \propto \tau_{lag}^{-1}$. On the other hand, Wu & Fenimore (2000) believed that the synchrotron cooling timescale in a magnetized jet is much shorter than the lag timescale. According to the internal shock model of GRBs (Rees & Mészaros 1994), there are three possible sources of time variation structure in GRB pulses: cooling, hydrodynamics, and geometric angular effects. Wu & Fenimore argued that cooling is much too fast to account for the observed lags and angular effects should be energy independent. Thus, only hydrodynamical processes are responsible for these lags. To be more precise, as magnetic fields and relativistic flows are likely to be involved in various ways, relativisitic magnetohydrodynamic (RMHD) processes (e.g., Lou 1992, 1993a, 1993b, 1994, 1996, 1998) might be relevant to the understanding these lags. Ioka & Nakamura (2001) argued that the pulse peak luminosity-variability relation might be caused by the variation in viewing angle of the source jet. The correlation between pulse lag or luminosity and jet-break time was noticed by Salmonson & Galama (2002), first revealing a connection between a feature of the GRB phase and the afterglow phase. The correlation may be qualitatively understood from models in which the Lorentz γ factor of an RMHD jet decreases as a function of angle away from the jet axis. Kocevski & Liang (2003) established empirically the connection between the GRB spectral evolution rate and spectral lag. They suspected that this may eventually reveal the underlying physical mechanism(s) for the spectral lag-luminosity correlation.

As has been suspected, the spectral lags of GRBs and their evolution are vital to probe the physics of GRB. We do want to know whether the lag-luminosity relation remains to be a universal feature for GRBs. In fact, Sazonv, Lutovinov & Sunyaev (2004) have found that the peak luminosities of GRBs 031203 and 980425 measured from the given cosmological parameter and redshift z are much lower than ones expected with lag-luminosity relation. Perhaps, only a certain kind of GRBs (e.g., those not associated with SNe) fit in the lag-luminosity relation. We would also like to know whether there are cases of negative lags in long GRBs. Previous observations of spectral lags were usually based on the data with a relatively low time resolution, such as the data acquired in the Discriminator Counts (DISCSC) mode of BATSE, with a time resolution of 64ms. As most spectral lags in time are fairly small, typically ≤ 100 ms, an analysis of spectral lag properties using 64ms time bin data would appear somewhat coarse and insufficient. In contrast, the TTS mode data of BATSE provides an opportunity to determine more precise temporal structures of GRB spectral lags. To resolve more fine spectral lag information from TTS mode data (e.g. lags less than 64ms) and especially to examine the distribution and evolution of the spectral lags are the major tasks we would like to pursue in this research work.

This paper is structured as follows. Observations and data analyses are described in §2. The results are presented in §3. In §4, we summarize the conclusions and provide discussions.

2. Database

The BATSE data acquired at both the TTS mode and the DISCSC mode were taken in the following four photon energy bands: 25-55 keV, 55-110 keV, 110-320 keV and >320 keV. The two data acquisition modes of operation are fundamentally different: The TTS mode records the time interval for every 64 γ -ray photons, while the DISCSC modes provides the number of γ -ray photons in every 64ms time interval.

As we would like to infer and estimate spectral lags with a time resolution less than 64ms for individual pulses of a GRB, we interpolate the light curves obtained in the TTS mode with a temporal subinterval of 8ms resolution under the key assumption that these 64 photons distribute more or less evenly within each time interval of TTS mode of operation. The empirical reason of binning data into 8ms is that the resulting light curve with such a bin size is fine enough to achieve a reasonable level of signal-to-noise (S/N) ratio. In order to empirically justify the validity of such a temporal interpolation scheme, we have first determined the spectral lags of a dozen GRBs based on the data of both TTS and DISCSC modes for comparison with time lags longer than 150 ms. The results are mutually consistent within estimated error bars.

The procedure of estimating spectral lags of GRBs using a cross-correlation function (CCF) has been widely adopted (e.g., Link et al. 1993; Fenimore et al. 1995; Norris et al. 2000). The CCF of $x_1(t)$ and $x_2(t)$ for the time duration of each pulse of GRBs, where $x_1(t)$ and $x_2(t)$ are respective light curves in two different γ -ray photon energy bands (namely, energy band I: 25 – 55

keV and energy band II: 110 - 320 keV), is simply defined by

$$CCF(\tau : \nu_1, \nu_2) = \frac{\langle \nu_1(t+\tau)\nu_2(t) \rangle}{\sigma_{\nu_1}\sigma_{\nu_2}},$$
(1)

where $\nu_i(t) \equiv x_i(t) - \langle x_i(t) \rangle$ is the light curve of zero mean and $\sigma_{\nu_i} \equiv \langle \nu_i^2 \rangle^{1/2}$ is the standard deviation away from the mean. The spectral lag time τ is defined as such to maximize the CCF($\tau; \nu_1, \nu_2$). A positive τ corresponds to an earlier arrival or leading higher-energy γ -ray photons. In order to reduce scattering of noises in the CCF, we use a Gaussian function with an additional linear term to fit the part around the peak of the CCF; in comparison, Norris et al. (2000) used quadratic as well as cubic fits. The fitting range is chosen based on (1) a sufficiently long length such that fits are always convergent and (2) a reasonably short length such that peaks are well identified and fit by relatively simple functions. Uncertainties of lags are determined by estimating errors transferred via the fitting parameters. As the fitting code can provide a 1σ parameter uncertainties, we calculate τ' for the fitting curves with parameters adding or subtracting 1σ uncertainties. The error in τ is thus defined as the maximum of the absolute difference between τ and τ' . On the theoretical ground, error bars should be greater than the time resolution of the data, that is, greater than 8ms and 64ms for the TTS and DISCSC data, respectively. Spectral lags calculated for the TTS and DISCSC data of a dozen GRBs with lags > 150ms do show consistency within estimated error bars.

The determination of a pulse duration time is equivalent to an estimation of the pulse width. However, it is not trivial to approach this problem simply by a code simulation. While the pulse temporal evolution of a GRB has often been described by a fast rise followed by an exponential decay (FRED) profile (e.g., Fishman et al. 1994; Fenimore 1999), there are other fitting profiles such as stretched exponentials, Gaussian (Norris et al. 1996), power-law decays (Ryde & Svensson 2000) or even some irregular shapes. For those GRB pulses with relatively 'standard' profile, we adopt the following model to fit their light curves, namely

Model I:
$$y(t) = y_0 + A \left\{ \exp \left[\frac{-(t - t_{max})}{\sigma_r} \right] - \exp \left[\frac{-(t - t_{max})}{\sigma_d} \right] \right\},$$

where y_0 is a background offset, t_{max} is the time of the pulse's maximum intensity, A; σ_r and σ_d represents the exponential rise ($t < t_{max}$) and decay ($t > t_{max}$) time constants, respectively [see eq. (1) in Norris et al. 1996], and

Model II:
$$y(t) = \frac{A}{w(\pi/2)^{1/2}} \exp\left[\frac{-(t - t_{max})^2}{2w^2}\right] + a + bt + ct^2$$
,

where y(t) is a Gaussian function with a quadratic term representing a background, t_{max} and A are similar to those in Model I and w, a, b, c are four fitting parameters. Model I has been applied for a GRB with a FRED profile, while Model II is more suitable for a GRB with a symmetric profile. In these two types of profile models, a GRB profile can be seen as a peak component superposed onto a background of either a constant y_0 (Model I) or a quadratic fit $a + bt + ct^2$ (Model II). With

a statistical weight of $w_i = 1/y_i$, we fit the TTS data for GRBs, taking the pulse width measured 0.1σ above the background $(y_0 \text{ or } a+bt+ct^2)$ (see Fig.1). For those GRB pulses of irregular shapes, we determine their pulse widths by direct visual examinations.

3. Results of Data Analysis

3.1. Distribution of Spectral Lags in Time

Several thousands of GRBs have been observed by BATSE/CGRO. As we plan to analyze the evolution of pulse spectral lags of long GRBs, we chose those GRBs with well separated multi-pulse profiles and good S/N ratios. A sample of 64 multi-peak long GRBs have been carefully selected from the TTS data. We calculate the spectral lags in time for every individual pulse of the selected sample. From the left to right columns in order, Table 1 lists the GRB trigger number according to the 'BATSE Catalog', the numeral identification of individual pulse in each GRB event, the pulse peak time (or position) of the low-energy band 25-55 keV, the peak count rate of the low-energy band 25-55 keV, the peak count rate of the high-energy band 25-55 keV, and the inferred spectral lags in time, where the peak count rate is determined by the average of three bins around the maximum. Due to the presence of a Poisson background variation in the light curve, we note that the sign of a lag does not necessarily always accord with that of the difference between the peak times of high and low energy bands.

The histogram of spectral lags for 341 pulses in 64 GRBs has a distinctly asymmetric sharp peak-like distribution as displayed in Figure 2. Also seen from Figure 2 is the important fact that shorter lags are much more numerous than longer lags. A large majority of spectral lags clearly show earlier arrivals of γ -ray photons in the high-energy band, with the maximum lag distribution at $\tau \sim 30 \text{ms}$. In contrast, only some 20 long GRBs show negative lags for which the absolute values are greater than their errors. Among these cases, there are 10 and 5 lags reaching 2σ and 3σ significant levels, respectively. While most spectral lags are positive, those negative spectral lags, if further confirmed to be real, would become additional constraints on physical models for GRBs. We have carefully examined those negative lags greater than 2σ significant level one by one to make sure that such negative lags are not caused by pulse overlaps. There are two major situations where negative spectral lags may arise. One situation usually occurs at the beginning of a GRB, such as the two GRBs 6333 and 7247, while the other situation happens as spectral lags vary gradually from positive to negative ones, such as the GRBs 5773 (see Fig. 3), 7277 and 7301. The GRB 6672 is an exception: it began with a positive spectral lag, then negative lags appeared, but returned to positive lags again in the end. Sometimes, the lag of the first pulse in a GRB cannot be well determined for the trigger time is not really at the beginning of the burst.

Gupta, Gupta & Bhat (2002) have studied spectral lags for GRBs of short durations. They observed in a sample of 156 BATSE GRBs with T90 (i.e., 90% of the duration time of a GRB) less

than 2s. Unlike GRBs of longer durations in our data analysis, they found the percentage of short GRBs with negative τ_{lag} is $\sim 26\%$, which is much higher than our result – only 10 and 5 negative spectral lags reaching above 2σ and 3σ level respectively among 341 pulses. Meanwhile, over 70% of short GRBs in their data sample have positive spectral lags in pulses. These significantly different distributions in positive and negative pulse spectral lags imply that there might be entirely different physical mechanisms responsible for long and short GRBs. It should be clearly noted that in estimating spectral time lags, there is an algebraic sign difference between our notation and that of Gupta et al. (2002) (i.e., our positive lags are their negative lags and vice versa).

3.2. Temporal Evolution of Spectral Lags

We can hardly see any systematic evolution of spectral lags. In other words, GRB spectral lags differ from each other in great varieties. The spectral lags of most GRBs do not change in the order of magnitude. However, a few of them varied significantly (e.g., GRBs 5773 and 6672). Some GRBs show their spectral lags increase (e.g., GRBs 4350 and 5548) or decrease (e.g., GRB 5773) regularly with increasing time. Considering the different physical mechanisms for GRBs (e.g., Piran 1999; Mészaros 2002), this dissimilarity in the evolution of GRB lags is not strange.

To give a graphic description, we present in Figure 4 spectral lags versus peak count rates for those long GRBs with more than 9 pulse peaks, where the count rates are the sum of those in the energy bands I and III.

As shown by Figure 4, relations between the count rates and the spectral lags are diverse. For example, in the case of GRB 7113, the spectral lags remain almost constant for different count rates. On the other hand, the spectral lags in GRBs 6124, 6587, 7277 and 7975 increase with decreasing count rates. Counter examples of such trend of variation do exist: the spectral lags of GRBs 7605 and 7954 tend to increase with increasing count rates. There seems to be no apparent relation between spectral lags and luminosity in general for pulses within a given long GRB.

4. Conclusions

We have calculated the spectral lags in time in pulses of 64 long GRBs using the TTS data of the BATSE/CGRO in the two γ -ray photon energy bands 25-55 keV and 110-320 keV. For the majority of pulses in GRBs, we see clear signals of earlier arrivals of high-energy γ -ray photons, with a spectral lag distribution peaked at a lag time of $\tau \sim 30 \text{ms}$. However, a few pulses do show negative lags, that is, lower-energy γ -ray photons arrived earlier than higher-energy γ -ray photons for pulses in a GRB event. While we cannot provide a rigorous statistical test for these negative lags as we do not know the actual distribution of spectral lags, the existence of such negative spectral lags in time for pulses in GRBs appears to be significant enough.

The dependence of the peak count rates on spectral lags varies significantly on the basis of individual GRB event.

Several GRBs show that their spectral lags either increase or decrease regularly with increasing time. Wu & Fenimore (2000) argued that time lags between different energy γ -ray photons might be mainly determined by the relevant dynamical timescale. Such regular and systematic changes in a GRB may be caused by some special processes associated with the shell ejecta movement. Based on our data analysis, we note that there is no strong evidence for a general correlation between spectral lags and luminosities to hold for pulses within a given GRB event. Although only one case, Hakkila & Gilblin (2004) noted that the peak luminosity ratio between two peaks of GRB 5478 is not in agreement with the ratio predicted by the lag versus peak luminosity.

We are grateful to the anonymous referee for a careful reading of several versions of this manuscript and for encouragement, constructive criticisms, valuable suggestions and helpful comments to improve the manuscript. This work has been partially supported by the National Science Foundation of China (NSFC 10273010) and by the State Basic Science Research Projects of China (TG20000776). Y.Q.L. has been supported in part by the ASCI Center for Astrophysical Thermonuclear Flashes at the Univ. of Chicago under Department of Energy contract B341495, by the Special Funds for Major State Basic Science Research Projects of China, by the THCA, by the Collaborative Research Fund from the National Natural Science Foundation of China (NSFC) for Young Outstanding Overseas Chinese Scholars (NSFC 10028306) at the NAOC, Chinese Academy of Sciences, by NSFC grant 10373009 at the Tsinghua Univ., and by the Yangtze Endowment from the Ministry of Education at the Tsinghua Univ. Affiliated institutions of Y.Q.L. share this contribution.

REFERENCES

Band, D. L. 1997, ApJ, 486, 928

Band, D. L., Norris, J. P., Bonnell, J. T. 2003, BAAS, 34, 1243 (astro-ph/0312336)

Cheng, L. X., Ma, Y. Q., Cheng, K. S., Lu, T., Zhou, Y. Y. 1995, A&A, 300, 746

Dai, Z. G., Liang, E. W., Xu, D. 2004, ApJ, 612, L101

Fenimore, E. E., in't Zand, J. J. M., Norris, J. P., Bonnell, J. T., Nemiroff, R. J. 1995, ApJ, 448, L101

Fenimore, E. E. 1999, ApJ, 518, 375

Fenimore, E. E., Ramirez-Ruiz, E. 2000 (astro-ph/0004176)

Fishman, G. J., et al. 1994, American Institute of Physics Conf. Proc. (AIPC), 307, 648

Gupta, V., Gupta, P., Bhat, P. N. 2002 (astro-ph/0206402)

Hakkila, J., Giblin, T. W. 2004 (astro-ph/00403360)

Ioka, K., Nakamura, T. 2001, ApJ, 554, L163

Kocevski, D., Liang, E. 2003, ApJ, 594, 385

Link, B., Epstein, R. I., Priedhorsky, W. C. 1993, ApJ, 408, L81

Lou, Y.-Q. 1992, ApJ, 397, L67

Lou, Y.-Q. 1993a, ApJ, 414, 656

Lou, Y.-Q. 1993b, ApJ, 418, 709

Lou, Y.-Q. 1994, Ap&SS, 219, 211

Lou, Y.-Q. 1996, MNRAS, 279, 129

Lou, Y.-Q. 1998, MNRAS, 294, 443

Mészaros, P. 2002, ARA&A, 40, 137

Murakami, T., Yonetoku, D., Izawa, H., Ioka, K. 2003, PASJ, 55, L65

Niemeyer, J. C., Truran, J. W. 2000, eds. Type Ia Supernovae: Theory and Cosmology, Cambridge University Press, United Kingdom

Norris, J. P., Nemiroff, R. J., Bonnell, J. T., Scargle, J. D., Kouveliotou, C., Paciesas, W. S. 1996, ApJ, 459, 393

Norris, J. P., Marani, G. F., Bonnell, J. T. 2000, ApJ, 534, 248

Norris, J. P. 2002, ApJ, 579, 386

Norris, J. P. 2003, Invited talk at the JENAM minisymposium on physics of GRB, Budapest, Hungary (astro-ph/0312277)

Phillips, M. M. 1993, ApJ, 413, L105

Piran, T. 1999, PhR, 314, 575 (Physics Reports, Vol. 314, Issue 6, pp 575-667)

Rees, M. J., Mészaros, P. 1992, MNRAS, 258, 41

Rees, M. J., Mészaros, P. 1994, ApJ, 430, L93

Salmonson, J. D. 2000, ApJ, 544, L115

Salmonson, J. D. 2001, AIPC, 586, 632

Salmonson, J. D., Galama, T. J. 2002, ApJ, 569, 682

Sazonov, S. Y., Lutovinov, A. A., Sunyaev, R. A. 2004, Nature, 430, 646

Schaefer, B. E. 2004, ApJ, 602, 306

Schaefer, B. E., Deng, M., Band, D. 2001, ApJ, 563, L123

Wu, B., Fenimore, E. E. 2000, ApJ, 535, L29

Fig. 1.— Upper panel: Two light curves of γ -ray photon energy bands I and III of GRB 4350. Three pulses can be clearly identified in this GRB event and the higher energy γ -ray photons lead the lower ones (i.e., positive spectral lags). Lower panel: Each pulse may be well fit by Model I. The procedure of determining the width of a pulse is also shown here.

This preprint was prepared with the AAS LATEX macros v5.2.

Fig. 2.— The histogram for spectral lags of all 341 pulses in 64 GRBs of BATSE/CGRO data acquired in the TTS mode. Positive spectral lags indicate earlier arrivals of higher-energy γ -ray photons. The two energy bands of γ -ray photons are 25-55 keV and 110-320 keV, respectively.

Fig. 3.— Two light curves of γ -ray photons in energy bands I and III of GRB 5773. Four pulses can be readily identified in this GRB event. The spectral lags change from positive to negative as can be seen by a direct visual inspection.

Fig. 4.— Variations of count rates versus spectral lags in time for 12 multi-pulse GRBs of BATSE/CGRO in the TTS mode. The numeral marked at one appropriate corner in each panel is the trigger number of that GRB given by 'The BATSE Catalog Burst Name'.

Table 1. Spectral Lags of GRBs of $\mathit{BATSE/CGRO}$ in the TTS Mode

GRB Trigger	Pulse	Peak 1	Peak Rate 1	Peak 2	Peak Rate 2	Spectral Lag
Number	ID (i)	Position (s)	(counts/s)	Position (s)	(counts/s)	in Time (ms)
	12 (1)	1 00101011 (0)	(6541165/5)	1 00101011 (0)	(65 dires)	Time (ine)
143	1	1.26	46704.09	1.22	137143.75	60.8 ± 11.2
	2	2.39	43109.49	2.32	116417.9	44.8 ± 8.96
	3	4.62	35436.35	3.72	92801.71	49.6 ± 8
	4	5.13	29438.69	5.1	77592.85	32.64 ± 8
	5	7.7	18834.17	7.7	27545.6	27.2 ± 8
	6	8.78	23030.62	8.77	37565.68	32 ± 8
	7	48.46	20298.77	48.42	33988.35	51.2 ± 8
	8	53.09	12500.69	52.74	13794.32	112.64 ± 8.96
219	1	113.71	9427.04	113.98	13191.89	448 ± 54.4
	2	116.17	20678.17	115.72	41205.2	471.36 ± 54.08
	3	119.91	14846.08	119.35	21079.44	478.4 ± 15.6
	4	127.76	8229.48	127.52	6275.81	438.08 ± 57.2
	5	131.93	7239.85	132.04	5768.08	424 ± 16
	6	134.15	8348.71	133.82	6385.35	435.2 ± 12.96
222	1	0.25	5444.67	0.54	5325.27	82.66 ± 22.04
	2	1.42	6164.05	1.33	6051.12	127.44 ± 104.04
	3	61.98	5371.59	62.23	4506.68	263.2 ± 28
	4	69.05	7433.04	68.75	9036.54	234.75 ± 8
249	1	15.3	14463.06	14.23	18077.19	64.64 ± 10.24
	2	18.98	27320.19	19.02	60113.95	-5.76 ± 8
	3	21.96	39382.03	21.26	93848.28	107.52 ± 8
	4	25.02	26597.9	25.02	43470.93	33.28 ± 16.64
	5	32.24	13462.76	32.1	13356.52	120 ± 12
	6	41.48	9394.71	42.68	8170.37	252.8 ± 8.8
612	1	5.16	4827.79	5.34	5830.81	144 ± 16.8
	2	8.35	5837.57	7.84	7831.93	102.4 ± 19.2
	3	10.71	5723.82	10.42	6294.77	308.42 ± 32.86
678	1	0.94	7418.09	0.87	20105.52	$64.29 \pm\ 21.25$
	2	0.94	7418.09	0.87	20105.52	68 ± 78
	3	1.51	8440.53	1.42	23727.88	0 ± 8.13
	4	4.72	7413.53	4.7	16477.24	-7.87 ± 11.81
	5	6.04	7125.27	5.99	13956.33	25.4 ± 8
	6	6.65	7897.96	6.53	16235.25	15.75 ± 8
	7	7.55	7274.85	7.7	14807.79	63.74 ± 10.62
	8	9.39	8316.6	9.34	16141.58	39.51 ± 8
	9	10.91	7915.53	10.82	16109.92	72.8 ± 8
	10	13.38	6987.72	13.47	10829.17	42.05 ± 14.02
	11	18.27	6483.86	18.18	7221.36	67.2 ± 8
841	1	2.18	6347.55	1.89	3711.56	80.64 ± 8
	2	12.28	8788.98	12.19	9610.47	76.74 ± 8
	3	15.01	6796.78	13.98	5130.81	117.6 ± 8.4
	4	16.99	5371.46	16.78	3672.38	151.2 ± 11.2
869	1	16.95	4094.31	17.98	5931.28	142.53 ± 16.77
	2	96.1	5089.73	94.95	6021.75	117.6 ± 19.6
	3	110.78	5478.87	110.97	7979.88	336 ± 16.8

Table 1—Continued

GRB Trigger	Pulse	Peak 1	Peak Rate 1	Peak 2	Peak Rate 2	Spectral Lag
Number	ID (i)	Position (s)	(counts/s)	Position (s)	(counts/s)	in Time (ms)
973	1	3.02	8807.73	2.18	12537.31	651.2 ± 10.4
0.0	2	23.41	7051.8	24.56	7036.9	112 ± 11.2
1025	1	0.06	6741.27	0.24	6313.29	60.16 ± 33.12
	2	1.65	10658.4	1.65	13611.31	5.28 ± 8
	3	2.13	14688.1	2.02	23291.17	70.4 ± 12.8
1085	1	3.9	13195.1	1.83	29906.9	474.24 ± 74.24
	2	6.5	24122.74	5.75	41496.01	752 ± 46
	3	7.6	19972.91	7.39	20160.15	172.8 ± 44.8
1190	1	0.17	4890.6	0.11	5134.78	28.8 ± 26.4
	2	0.34	5561.23	0.31	5340.42	27.58 ± 28.42
	3	0.82	5444.33	0.87	6402.98	28.0 ± 8
	4	2	5080.79	1.9	5751.9	33.6 ± 8
	5	2.92	4213.65	2.86	3724.16	29.5 ± 8
1204	1	0.09	5554.46	0.12	9852.05	-0.96 ± 8
	2	0.99	4407.6	1	4956.15	7.87 ± 8
	3	2.98	4298.2	2.9	3788.45	78.91 ± 11.9
4350	1	0.64	9804.3	0.71	7391.88	196 ± 14
	2	17.13	7058.09	13.69	7101.72	344.8 ± 17.28
	3	34.59	6380.98	33.67	4934.64	416 ± 56
5447	1	6.59	10676.96	6.9	5087.84	96 ± 9.6
	2	13.63	7045.25	13.25	3737.58	207.2 ± 14.4
5548	1	16.87	8533.64	16.9	10107.59	16.0 ± 8
	2	51.14	6082.37	50.42	6166.6	159.04 ± 10.08
	3	101.5	4548.6	101.51	3138.83	254.4 ± 25.2
	4	163.47	4564.25	166.1	3556.31	358.4 ± 12.8
5568	1	0.75	5865.03	0.86	8639.73	82.66 ± 39.95
	2	1.9	11073.6	1.83	34474.03	62.88 ± 48.96
FFE0	3	2.75	12678.03	2.74	32657.64	-10.4 ± 8
5572	1	0.17	11380.6	0.02	14793.24	-1.92 ± 8
	$\frac{2}{3}$	$0.77 \\ 4.22$	15103.77	0.76	28440.03	5.64 ± 8
5575	1	0.3	11405.69 11065.87	4.54 0.23	10612.42 15611.22	-3.36 ± 15.12 144.64 ± 13.44
9979	$\frac{1}{2}$	6.68	6076.13	6.02	5046.16	96 ± 16
	3	8.68	10190.02	8.58	11250.84	90 ± 10 44.35 ± 8
	4	9.22	11655.85	9.25	9916.92	72.11 ± 8
	5	9.96	11351.2	9.23	10029.7	80 ± 20.8
5591	1	51.22	5122.53	50.76	5015.69	289.6 ± 12
0031	2	100.25	5690.69	99.92	5648.2	185.6 ± 9.6
	3	144.13	6561	143.83	5631.88	240 ± 24
5601	1	4.47	5476.04	2.37	5029.91	563.6 ± 96.6
0001	2	7.4	7002.75	7.13	9498.09	460.1 ± 55.8
5621	1	3.49	11212.87	3.49	14532.77	29.44 ± 8
0021		0.10	11212.01	0.40	1 1002.11	20.11 ± 0
		3.92	19020.7	3.91	36243.95	54.5 ± 8
	2 3	$3.92 \\ 5.74$	$19020.7 \\ 12989.42$	3.91 5.74	36243.95 17888.9	54.5 ± 8 25.6 ± 8

Table 1—Continued

GRB Trigger	Pulse	Peak 1	Peak Rate 1	Peak 2	Peak Rate 2	Spectral Lag
Number	ID (i)	Position (s)	(counts/s)	Position (s)	(counts/s)	in Time (ms)
Nulliber	ID (I)	FOSITION (S)	(counts/s)	FOSITION (S)	(counts/s)	m rime (ms)
	5	7.14	13461.48	7.18	22535.45	60.48 ± 8
	6	9.98	9988.35	9.95	9078.3	-2.4 ± 8
5628	1	6.91	7630.21	7.18	9852.22	-6.4 ± 43.2
	2	7.7	8090.29	7.71	11792.75	40 ± 8
	3	9.03	8091.89	9.01	10009	-2.82 ± 8
	4	10.06	10466.05	10.2	15583.61	21.7 ± 8
5654	1	21.18	6542.94	14.62	9984.46	499.2 ± 76.8
	2	33.65	5905.52	37.66	6685.05	167.84 ± 23.92
	3	78.34	4844.36	77.74	3532.31	104.8 ± 61.2
	4	92.96	4401.31	92.72	3812.54	345.6 ± 25.6
5726	1	3.47	6173.52	3.38	4185.61	112 ± 14
	2	5.38	6131.64	5.03	6228.25	62.09 ± 8
	3	7.37	7520.29	6.98	7547.79	36.48 ± 8
5729	1	28.41	7541.93	27.98	4970.05	372.74 ± 13.31
	2	38.68	8518.49	36.78	5705.94	585.73 ± 39.94
5731	1	14.25	6106.97	14.03	6032.85	89.86 ± 8
	2	34.31	6040.33	34.12	7833.2	84 ± 8
	3	38.69	6479.97	38.58	7496.68	99.2 ± 8
5773	1	11.34	11345.14	8.11	18127.99	1256.2 ± 78.4
	2	17.72	16424.96	16.87	19671.89	195.2 ± 15.6
	3	23.52	11741.22	24.32	7372.24	140.2 ± 25.4
	4	33.66	8780.13	35.18	5233.09	-364.42 ± 14.02
5989	1	0.38	69045.97	0.27	110138.38	70.4 ± 8
	2	1.1	21951.07	1.03	8125.8	68.88 ± 8
	3	18.7	15184.64	18.58	7545.06	39.51 ± 8
	4	20.48	28495.33	20.36	11093.89	64.92 ± 8
	5	23.78	30222.18	23.54	7458.01	78.72 ± 8
6100	1	6.37	11256.17	6.21	21148.39	84.1 ± 10.51
	2	8.31	15987.26	8.31	33571.85	69.76 ± 8
6124	1	1.18	14047.67	1.14	32134.29	139.2 ± 8
	2	6.12	18155.54	6.1	42918.34	18.05 ± 8
	3	7.34	17233.61	7.08	39099	20.4 ± 8
	4	8.22	16553.99	8.64	54925.32	22.5 ± 8
	5	9.34	21629.41	9.42	66180.71	19.76 ± 8
	6	10.02	19731.38	10.02	72543.17	11.25 ± 8
	7	11.3	16476.98	11.29	49369.37	10.08 ± 8
	8	12.77	21607.11	12.76	72135.56	11.2 ± 8
	9	14.86	15829.08	14.78	27685.85	46.77 ± 8
6157	1	0.94	6198.38	0.89	8506.09	35.58 ± 8
	2	2.27	6522.94	2.13	11378.44	45.63 ± 14.88
	3	2.54	6661.34	2.59	10456.45	46.77 ± 9.74
	4	3.39	6029.75	3.42	11717.95	27.78 ± 8
	5	4.46	10397.08	4.48	20453.35	18.08 ± 8
	6	5.91	6587.55	6.06	13462.95	39.36 ± 8
	7	6.39	5681.97	6.4	10786.04	0.57 ± 142.91

Table 1—Continued

GRB Trigger	Pulse	Peak 1	Peak Rate 1	Peak 2	Peak Rate 2	Spectral Lag
Number	ID (i)	Position (s)	(counts/s)	Position (s)	(counts/s)	in Time (ms)
	8	7.21	9376.81	7.18	19577	63.17 ± 8
	9	8.8	5467.62	8.81	5430	44.44 ± 8
	10	9.15	6066.33	9.11	11111.71	16.93 ± 8
6168	1	25.2	9263.25	25.11	15846.34	144 ± 16.8
	2	27.54	12669.29	27.27	30621.96	108.99 ± 41.92
6333	1	1.54	6801.92	1.89	4335.05	-347.12± 26.52
	2	4.97	7257.69	5.01	5313.64	43.39 ± 8
	3	6.39	7056.58	6.43	4654.19	3.36 ± 11.76
6336	1	4.36	9241.58	4.46	19402.64	18.24± 21.89
	2	5.4	13560.22	5.18	29018.18	239.68 ± 15.84
	3	6.71	11840.69	6.38	12467.35	-11.29 ± 14.11
6404	1	3.48	19305.13	3.43	36109.4	246.4 ± 8
	2	8.73	25334.39	8.54	34959.45	123.2 ± 12
	3	38.42	6196.4	38.06	4875.59	229.6 ± 19.6
	4	40.43	6802.02	40.15	5109.6	209.98 ± 18.53
6554	1	0.62	5432.32	0.23	4483.81	601.6 ± 33.6
	2	8.9	6558.73	9.02	3394.91	14.02 ± 8
6560	1	0.56	8513.42	0.17	9543.97	34.4 ± 8
	2	1.21	6045.44	1.48	3818.73	56.45 ± 79.03
	3	4.19	7594.62	4.14	9639.94	63.84 ± 8
	4	16.98	8918.76	17.28	13295.21	112.9 ± 8
	5	17.58	8604.36	17.34	17355.12	185.15 ± 34.27
	6	17.87	8850.72	17.77	14587.61	112.32 ± 47.04
	7	22.7	9828.27	22.95	12401.11	72 ± 43.68
	8	23.5	11299.79	23.35	19121.28	70.16 ± 8
	9	24.25	10132.65	24.46	15807.05	84.67 ± 14.78
	10	25.89	12569.71	25.84	16564.29	77.38 ± 8
	11	29.08	11165.58	29.02	9849.95	115.72 ± 8
	12	35.13	7388.69	35	9025.26	202.24 ± 8
6587	1	10.13	9493.22	9.7	19390.77	88 ± 29.44
	2	11.25	11099.49	10.92	15888.32	138.69 ± 8
	3	11.87	11200.93	11.7	11877.43	94.08 ± 72.24
	4	13.81	14157.62	13.58	30840.62	63.36 ± 8.45
	5	14.97	12111.7	15.05	27281.2	14.11 ± 8
	6	16.81	14243.11	16.94	35134.52	61.6 ± 11.2
	7	21.5	15612.32	20.68	41642.4	0 ± 11.23
	8	22.69	11547.73	22.73	36169.06	10.9 ± 8
	9	23.21	16687.85	23.18	42142.4	-6.72 ± 8.4
	10	24.78	17749.89	24.82	46530.71	22.4 ± 8
	11	26.11	13593.47	26.35	35845.33	9 ± 12.37
	12	27.53	18791.42	26.98	52804.52	-0.8 ± 8
	13	29.99	15973.07	29.94	40879.16	45.16 ± 8.47
	14	31.15	12667.77	31.1	21965.7	11.29 ± 8
6672	1	0.93	10997.34	0.87	9432.11	120.22 ± 9.25
	2	3.88	8699.88	3.86	4635.64	-99.2 ± 35.2

Table 1—Continued

GRB Trigger Number	Pulse	Peak 1 Position (s)	Peak Rate 1 (counts/s)	Peak 2	Peak Rate 2	Spectral Lag
Number	ID (i)	Position (s)	(counts/s)	Position (s)	(counts/s)	in Time (ms)
	3	7.25	8011.5	6.85	4869.85	27.84 ± 9.28
7113	1	3.37	14402.16	3.28	28654.04	65.09 ± 8
	2	6.51	17721.43	7.42	32685.95	24.1 ± 8
	3	8.78	17510.57	8.74	31280.82	4.51 ± 8
	4	12.03	19428.95	10.26	38888.76	10.54 ± 8
	5	16.69	23126.18	16.71	65265.06	-0.64 ± 8
	6	19.7	57515.45	19.74	69960.89	22.4 ± 8.4
	7	21.37	30765.45	21.36	54300.82	21.89 ± 8
	8	22.55	23176.57	22.92	41652.65	0.8 ± 8
	9	23.38	27241.76	24.1	61314.25	-12.2 ± 14.6
	10	24.65	26648.13	24.58	60490.65	-13.54 ± 8
	11	26.34	35474.09	26.34	83907.04	$9.54 \pm \ 8$
	12	28.06	23596.59	28.19	51085.72	-22.46 ± 8
	13	29.22	28968.98	29.22	62544.48	$8.47 \pm \ 8$
	14	31.11	37284.11	33.8	57153.23	5.8 ± 8
	15	35.38	26963.79	35.98	59132.34	25.0 ± 8
7185	1	5.49	6175.93	5.78	5385.61	100.8 ± 8
	2	53.18	6798.85	52.46	6463	182.4 ± 8
	3	67.7	7703.87	67.68	6414	294.53 ± 8
	4	69.89	7398.18	69.75	8126.25	252.8 ± 8
	5	74.99	6745.86	74.73	5792.94	190.08 ± 8.45
	6	86.06	7479.47	85.94	5315.92	228.8 ± 8
	7	90.67	5665.2	90.7	4376.22	224.35 ± 8
	8	107.66	6722.01	107.16	4076.01	386.4 ± 11.2
	9	110.09	7238.85	109.63	4458.83	276.67 ± 12.58
	10	131.69	5886.4	131.31	4664.4	476.8 ± 32
	11	134.63	7530.29	134.25	4752.98	630.72 ± 14.02
	12	141.51	6691.83	140.93	4029.32	456 ± 12
	13	148.04	10601.5	147.58	8035.55	441.6 ± 8
	14	155.62	6341.69	154.6	3846.78	427.58 ± 12.58
7240	1	0.66	6143.53	0.62	15187.18	5.85 ± 8
	2	3.02	9470.03	3.02	22659.87	39.04 ± 8
7247	1	13.83	4890.78	20.24	6322.53	-409.6 ± 64
	2	35.34	6156.84	35.2	10162.96	140.8 ± 9.6
7277	1	5.81	8330.56	5.62	7526.75	78.62 ± 11.23
	2	12.06	9470.15	11.91	8152.23	35.33 ± 11.78
	3	13.14	10034.39	13.11	8292.93	16.93 ± 8.47
	4	13.93	9891.21	13.94	8363.95	-28.16 ± 24.64
	5	15.56	9805.23	15.56	10040.36	-28 ± 8.4
	6	16.94	10139.89	16.9	10283.65	-8.38 ± 8
	7	23.52	10585.91	23.5	9677.3	11.9 ± 11.9
	8	24.32	10334.18	24.16	9153.41	-10.09± 8
	9	25.78	14267.59	25.73	12911.01	-15.74 ± 11.81
	10	27.94	10905.58	27.38	10817.12	-92.8 ± 32
7301	1	2.08	13211.36	3.3	15796.25	33.5 ± 8.1

Table 1—Continued

GRB Trigger Number	Pulse ID (i)	Peak 1 Position (s)	Peak Rate 1 (counts/s)	Peak 2 Position (s)	Peak Rate 2 (counts/s)	Spectral Lag in Time (ms)
	2	16.9	31436.79	16.67	90769.16	10.7± 8
	3	19.08	28238.96	19.09	79843.72	-21.9 ± 8
	4	32.45	13325.43	32.57	12153.23	-113.6 ± 8.4
7343	1	26.23	13877.48	25.34	35294.72	-113.0 ± 0.2 33.6 ± 16.8
1343	$\frac{1}{2}$	32.1		25.34 31.39	18137.39	
			9970.74			235.87 ± 8
	3	38.73	11990.98	38.3	29087.97	313.82 ± 22.42
TF 00	4	77.9	9681.45	76.88	11955.15	88 ± 36
7560	1	4.63	13276.4	4.83	14945.85	-5.11 ± 8
	2	6.61	10286.24	6.47	6738.54	-21.9 ± 12.2
	3	45.45	14452.45	45.22	19496.01	160 ± 8
	4	48.34	15433.98	47.94	20457.11	159.3 ± 8
	5	58.28	10509.12	58.25	6044.53	226.37 ± 8
	6	72.34	7915.58	71.73	5624.59	181.38 ± 17.44
7281	1	0.18	19313.04	0.08	35588.5	56.99 ± 56.48
	2	0.56	24548.62	0.56	29636.68	17.92 ± 8
	3	1.38	14841.34	1.39	11134.64	-5.71± 8
7592	1	1.1	28885.81	1.1	87186.68	12.8± 8
	2	2.42	21719.17	2.42	52149.73	25.6 ± 8
	3	25.54	19134.16	24.9	20753.14	568 ± 40.8
7605	1	1	6280.25	0.82	6372.43	47.2± 9.6
	2	2.06	7473.61	2.04	5608.95	79.03 ± 8
	3	2.84	6769.1	2.56	7014.72	109.66 ± 8
	4	5.09	6219.77	7.33	5920.6	65.0 ± 15.8
	5	10.47	7038.2	10.45	6106.67	25.34 ± 8.45
	6	12.55	6421.32	12.49	6028.94	67.07 ± 8
	7	13.91	7052.97	14.35	4542.31	-3.87 ± 33.9
	8	16.1	6217.25	16.07	6229.82	68.08± 8
	9	16.67	6533.59	16.86	6651.85	39.68 ± 11.9
7610	1	2.63	7641.71	2.54	8291.97	67.74± 8
7010	2	3.65	9039.63	3.79	10293.75	40.32 ± 8
	3	4.76	10056.44	4.7	21288.27	3.2 ± 8
FOE1	4	5.46	5542.52	5.45	9148.14	148.72 ± 22.12
7651	1	2.63	6889.28	2.44	8383.71	130.48 ± 13.5
	2	3.98	7423.85	3.55	10129.12	12.48 ± 21.6
	3	7.73	8513.08	7.49	8494.76	118.88± 8
	4	27.58	7887.49	27.42	6972.15	202.24 ± 23.04
	5	28.26	9172.29	28.21	11805.66	98.78 ± 8
	6	30.02	9383.27	29.71	9821.42	265.57 ± 15.44
	7	31.97	8674.51	31.66	9437.04	162.4 ± 8.4
	8	34.05	9159.45	33.9	12863.55	134.4 ± 8.4
7688	1	3.14	5021.42	4.09	6534.36	67.36 ± 12.96
	2	7.16	5773.21	6.75	10716.66	74.24 ± 10.24
	3	11.48	4919.93	11.02	7405.73	99.84 ± 15.36
	4	18.82	4765.4	18.62	6767.25	68.8 ± 8
7695	1	0.01	9997.59	0.14	34082.12	7.68 ± 8

Table 1—Continued

GRB Trigger Number	Pulse ID (i)	Peak 1 Position (s)	Peak Rate 1 (counts/s)	Peak 2 Position (s)	Peak Rate 2 (counts/s)	Spectral Lag in Time (ms)
	2	1.26	15184.9	1.26	47648.71	9.6 ± 8
	3	2.08	11189.21	1.93	28174.99	-0.93 ± 8
	4	2.26	12987.99	2.26	41957.11	6.38 ± 8
	5	4.14	15044.82	2.82	41102.16	-2.82 ± 8
	6	5.94	13755.44	5.94	39713.14	1.28 ± 8
	7	7.02	12637.03	7.09	26390.67	-6.4 ± 8
	8	9.15	8964.57	8.94	13251.85	2.56 ± 8
	9	9.9	8043.57	9.81	10469.08	-14.08± 8
	10	11.7	10652.57	11.76	18560.27	-10.88± 8
	11	13.89	8558.67	13.91	10525.66	-5.12 ± 8
	12	14.67	7621.24	14.46	11840.41	9.8 ± 8
	13	21.69	7419.13	21.81	8900.46	-26.88 ± 12.48
7906	1	17.26	27293.02	17.13	52387.8	154.18± 8
	2	20.58	62602.4	20.52	130010.53	92.22 ± 8.38
	3	22.71	62967.53	22.62	125032.32	78.72 ± 8
	4	25.72	29331.29	25.64	30459.1	140 ± 8
	5	26.82	28886.48	26.78	19976.09	89.38 ± 8
	6	29.68	49836.62	29.64	69791.91	59.36 ± 8
	7	31.3	51076.85	31.25	63184.7	93.44 ± 8
7925	1	9.99	8833.15	9.5	16207.43	192.0 ± 38
	2	28.32	6167.3	28.29	11008.93	81.85 ± 8
	3	30.42	6465.81	30.48	7932.42	13.6 ± 12.32
	4	31.15	6636.39	30.89	7807.2	104.4 ± 14.11
	5	87	7829.75	86.98	14396.44	441.6 ± 12.8
7954	1	0.85	18555.32	0.8	36346.06	48 ± 8
	2	1.23	15929.81	1.24	53627.18	13.76 ± 8
	3	9.45	30656.88	9.42	68396.69	60.48 ± 8
	4	10.14	22981.44	10.12	53973.07	41.92 ± 8
	5	10.73	31529.55	10.73	86100.83	37.76 ± 8
	6	12	10284.52	12	16411.95	-2.25± 8
	7	12.85	21002.68	12.84	32831.5	22.5 ± 8
	8	13.89	18092.25	13.89	34841.63	$47.24\pm\ 8$
	9	14.87	18788.42	14.81	45039.05	24.75 ± 8
7975	1	5.62	5948.9	4.24	5836.87	268.8 ± 43.2
	2	69.78	5117.93	69.9	5512.82	153.6 ± 8
	3	75.06	4831.78	74.44	4069.48	284.26 ± 15.79
	4	77.93	8232.47	77.89	11267.32	191.23 ± 10.62
	5	78.84	8207.79	79.46	9780.49	168.2 ± 54.7
	6	80.38	10760.89	80.14	15902.9	42.08 ± 8
	7	81.38	10250.06	81.14	13218	154.56 ± 8
	8	83.45	10295.42	83.31	10273.4	252.1 ± 12.93
	9	89.46	6073.21	89	5618.15	212.8 ± 8
	10	92.61	6771.17	92.41	6023.46	218.4 ± 8
	11	95.56	7030.29	95.44	6191.42	231.84 ± 13.44
	11	30.00				

Table 1—Continued

GRB Trigger	Pulse	Peak 1	Peak Rate 1	Peak 2	Peak Rate 2	Spectral Lag
Number	ID (i)	Position (s)	(counts/s)	Position (s)	(counts/s)	in Time (ms)
8022	1	2.83	8080.59	2.78	11553.08	107.84 ± 30.24
	2	3.38	6685.64	3.29	5216.47	-44.8 ± 39.2
	3	7.82	7066.22	7.36	4570.54	117.38 ± 8.38
	4	13.25	6304.86	13.74	4473.76	97.66 ± 17.44
8030	1	1.02	4732.8	0.95	7478.56	66.82 ± 8.35
	2	2.65	4164.49	2.63	3862.87	122.5 ± 8.45
	3	15.6	4580.29	15.62	7527.69	161.28 ± 8
	4	17.51	4492.37	17.14	6397.1	43.68 ± 8
	5	18.18	4500.05	18.14	4849.06	43.3 ± 11.81
	6	20.3	4983.15	20.31	10017.68	117.38 ± 8
8081	1	0.75	5776.88	0.71	6822.93	27.84 ± 8
	2	20.7	8202.56	20.75	10101.55	71.81 ± 8
	3	21.94	8494.25	21.9	11999.75	25.31 ± 8
	4	23.34	7230.99	23.26	5887.67	107.52 ± 8
8087	1	1.2	5204.05	1.3	5597.91	76 ± 34
	2	5.12	7713.57	5.1	11056.65	64 ± 8
	3	6.9	6259.22	6.5	8891.9	139.87 ± 8
	4	8.86	5572.11	8.72	8376.39	0 ± 8
	5	10.1	5753.64	10.03	7333.64	13.6 ± 16.72
	6	40	5275.8	39.66	4921.9	26.6 ± 11.4
8109	1	0.57	6507.3	0.23	7823.73	227.2 ± 8
	2	2.36	7943.62	1.26	10602.3	824.84 ± 68.2

Note. — From the left to right columns:

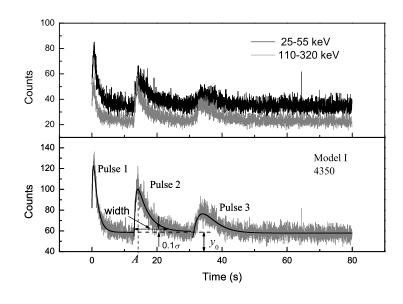
Column 1: the GRB trigger number tabulated in the 'BATSE Catalog';

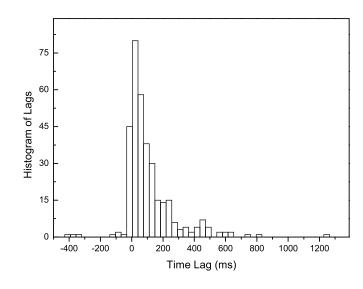
Column 2: the numeral identification of an individual pulse in each GRB event;

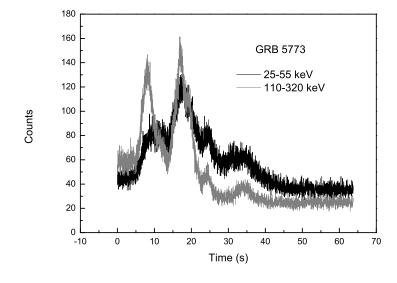
Columns 3 & 5: the pulse peak positions of the low-energy band $(25-55~{\rm keV})$ and of the high-energy band $(110-320~{\rm keV})$, respectively;

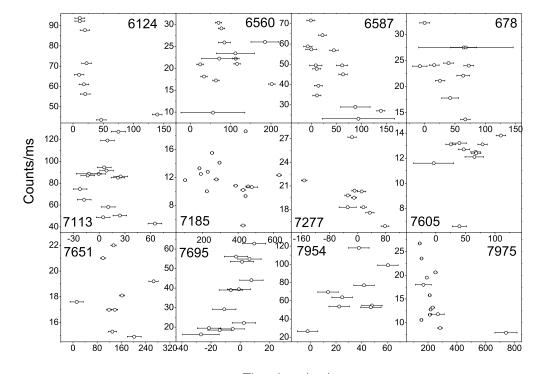
Columns 4 & 6: the peak count rates of the low-energy band and of the high-energy band, respectively, where the peak count rate is determined by the average of three bins around the maximum;

Column 7: the spectral lags with their error estimates.









Time Lag (ms)